

**INTERNATIONAL JOURNAL OF ENGINEERING SCIENCES & RESEARCH
TECHNOLOGY****OPTIMIZATION OF THE HEAT EXCHANGER IN A FLAT PLATE INDIRECT
HEATING SOLAR WATER HEATING SYSTEM****J. L. Pratyusha, Mr. N. Vasudeva Rao, Asst Professor**

Department of Mechanical Engineering, BVC Engineering college, India

DOI: 10.5281/zenodo.221117

ABSTRACT

Most of the modern day energy needs is being supplied by fossil fuels and these are consumed at such a rate that the reserves of oil and gas would last for not more than 250 years. If we try to see the implications of these limited reserves we will be faced with a situation in which the unit cost of energy will be high and concern about the environmental pollution caused by burning of the fossil fuels. Solar energy is one of the important renewable energy source and an important application in the water heating for domestic and industrial purposes. It incorporates the collection of a solar energy and hot water storage in one unit. The aim is to investigate the effect of different parameters on the thermal performance of this system with the aim of reducing both the initial and the running costs. The outlet service water temperature was used as a measure of performance, because it is an indicator of the energy acquired from the solar radiation. The continuity, momentum and energy equations of the fluids involved in the system were numerically solved in a steady state condition, using FLUENT software. Three-D CFD models were developed and validated using previous experimental results. A standard $k-\omega$ turbulent model was used in the optimization of the heat exchanger. The surface-to-surface radiation model was included. The effect of single and double row heat exchangers with different lengths investigated. Circular and elliptic cross-section pipes were also examined. Mass flow rates of 500 and 650 L/h were chosen. The results showed that the single row HX of 10.8 m length for both the elliptical and type B tube gave high service water outlet temperature and with low pumping power.

KEYWORDS: Solar Water Heating, FLUENT, Standard $K-\Omega$ Turbulent Model, Heat Exchanger**INTRODUCTION**

Energy resources are classified into two types: renewable resources including solar energy, wind power, hydraulic energy, geothermal energy and biomass energy, and non-renewable resources that cannot be replenished, such as petrol, nuclear energy, coal and natural gas. Figure 1.1 presents the world's energy consumption. The world's energy usage from non-renewable resources adds up to 91.88% while 8.12% of the energy is generated from renewable resources.

Fossil fuels, which are main source of energy, are getting depleted. As a consequence the cost of fossil fuels is increasing. Further, the fossil fuel based systems produce detrimental effects on the environments. This in turn will affect our health. Due to the massive increase in the non-renewable fuel prices and the increase in public awareness of its negative impact on the environment, the growth of renewable energy has accelerated over the past few years; power generated from renewable resources has increased to 14% of the total growth in global power generation. However, because of the enormous growth in the energy consumption, this growth is not enough to reduce the level of carbon emissions. As a consequence of the increase in the world's population, human development, the increase in individual income, and the aspiration for more comfortable life styles, the power consumption has increased significantly over the last three decades resulting in an increase in carbon emissions.

Increasing the investment of the clean resources involves four sectors: industrial, transportation, residential and commercial. The highest energy consumption occurs in the industrial sector. Therefore, much research has been conducted to reduce the energy consumption in this sector. The lowest consumption occurs in the commercial sector. The contribution of the present study will be in the residential sector. This study will focus on using the solar energy for domestic applications to reduce burning fossil fuel and hence carbon emission.

SYSTEM MODIFICATIONS USING THE CFD APPROACH

To evaluate the thermal performance of the indirect heating integrated collector storage solar water heating system, the velocity, temperature and pressure of the fluids involved in the system need to be evaluated. These fluids are water (in the storage tank and the service water in the pipe) and air (in the gap spacing between the glass covers). The equations that govern the fluid flow and heat transfer are the continuity, momentum and energy equations. The equations for unsteady, turbulent and incompressible flow are presented below.

1. The continuity equation can be written as

$$\text{div } \mathbf{U} = 0$$

Where;

\mathbf{U} : fluid velocity vector (i.e. $\mathbf{U} = \bar{u}i + \bar{v}j + \bar{w}k$)

The continuity equation is written in rectangular coordinates as below.

$$\frac{\partial \bar{u}}{\partial x} + \frac{\partial \bar{v}}{\partial y} + \frac{\partial \bar{w}}{\partial z} = 0$$

2. The momentum or Reynolds-Averaged Navier-Stokes equations are:

- a. x-momentum equation

$$\begin{aligned} \frac{\partial \bar{\rho} \bar{u}}{\partial t} + \text{div}(\bar{\rho} \bar{u} \mathbf{U}) \\ = - \frac{\partial \bar{p}}{\partial x} + \text{div}(\mu \text{grad} \bar{u}) \\ + \left[- \frac{\partial (\overline{\bar{\rho} u'^2})}{\partial x} - \frac{\partial (\overline{\bar{\rho} u' v'})}{\partial y} - \frac{\partial (\overline{\bar{\rho} u' w'})}{\partial z} \right] \\ + f_x \end{aligned}$$

b. y-momentum equation

$$\begin{aligned} \frac{\partial \bar{\rho} \bar{v}}{\partial t} + \operatorname{div}(\bar{\rho} \bar{v} \mathbf{U}) \\ = - \frac{\partial \bar{p}}{\partial y} + \operatorname{div}(\mu \operatorname{grad} \bar{v}) \\ + \left[- \frac{\partial(\bar{\rho} u' v')}{\partial x} - \frac{\partial(\bar{\rho} v'^2)}{\partial y} - \frac{\partial(\bar{\rho} v' w')}{\partial z} \right] \\ + f_y \end{aligned}$$

c. z-momentum equation

$$\begin{aligned} \frac{\partial \bar{\rho} \bar{w}}{\partial t} + \operatorname{div}(\bar{\rho} \bar{w} \mathbf{U}) \\ = - \frac{\partial \bar{p}}{\partial z} + \operatorname{div}(\mu \operatorname{grad} \bar{w}) \\ + \left[- \frac{\partial(\bar{\rho} u' w')}{\partial x} - \frac{\partial(\bar{\rho} v' w')}{\partial y} - \frac{\partial(\bar{\rho} w'^2)}{\partial z} \right] \\ + f_z \end{aligned}$$

SYSTEM MODIFICATIONS USING THE CFD APPROACH

The indirect heating system is the most economical solar water heating system. In this project, CFD approach was used to enhance the efficiency of the indirect heating system. The objectives of this study are to increase the heat gain from the sun, minimise the heat loss from the system, and reduce both the initial and operating costs. The optimum air gap size was investigated to reduce the heat losses to the ambient atmosphere through radiation and convection heat transfer. The optimum heat exchanger design was also investigated to enhance the heat gained by the service water. The chosen system has the following parameters:

1. Double glass covers with glass thickness of 3 mm
2. Absorber area of 0.7 m × 1.35 m with 10 mm thickness of metallic nickel chrome (M-N-chrome)
3. Storage tank volume of 81 x 135 x 10 cm (containing about 109l of water) with 2 mm thickness of iron sheet
4. Insulation walls of wood with 50 mm thickness
5. Copper service water tubes of 1 mm thickness.

The physical properties used in the simulation of these materials are given in Table 1.

Table:1

Physical properties of Material name	Density (ρ) kg/m ³	Specific heat (Cp) J/(kg. K)	Thermal conductivity (k) W/(m. K)	Emittance (ε)
M-N-chrome	7865	460	19	0.94
Glass	2800	800	0.81	0.93
Wood	700	2310	0.173	0.9
Copper	8978	381	387.6	Not included
Iron	7832	434	63.9	Not included

OPTIMISATION OF THE AIR GAP SPACING

The function of the air gap spacing is to insulate the absorber surface shown in figure 1. However, the effectiveness of this insulation depends on the size of the air gap spacing (Manz 2003; Mossad 2006). Thus, the choice of the size of these gaps will have an impact on the performance of the solar collector. The system chosen in this work has a double air gap spacing, because it was found to have an efficient thermal performance (Kumar & Rosen 2011). L1 is the lower air gap spacing between the absorber and the lower glass cover and L2 is the upper gap between the upper and lower glass covers. L1 and L2 were varied within the range of 15-50 mm to investigate which combination of gap sizes would result in minimum total heat losses; including radiation and convection

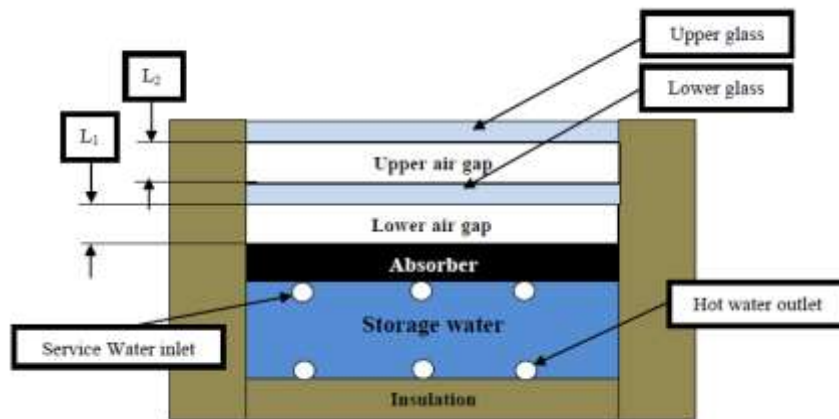


Figure 1. Cross section of the indirect heating integrated collector storage solar water heating system with double glass cover

CFD MODEL

3D CFD models for the absorber with the double glass cover (i.e. without the storage water and the heat exchanger) were developed to evaluate the radiation and convection losses. L1 was changed to 15, 25 and 40 mm. For each value of L1, L2 was changed to 15, 25, 35 and 50 mm (i.e. combinations of 12 cases were investigated). The geometry and the computational grid were generated, using ANSYS 13.0-Workbench. To validate the grid independency, three computational grids were developed for the model of L1 equals 25 mm and L2 equals 50 mm for 100,000, 162,000 and 227,500 elements. The elements shape were hexahedral for all models and finer mesh was chosen close to the walls. The 162,000 and 227,500 elements provided the same results which had 1 to 1.5% differences from the results of the 100,000 model.

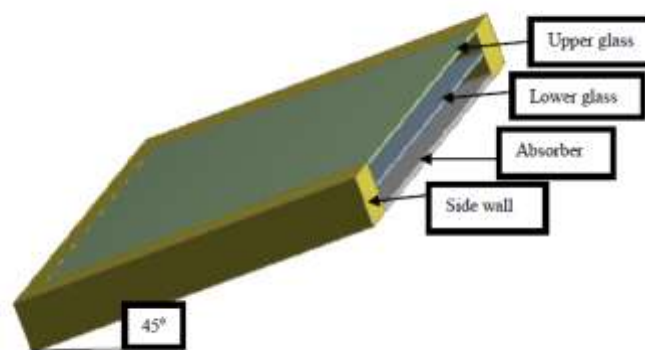


Figure 2. 3D model of the air spacing of the integrated collector system

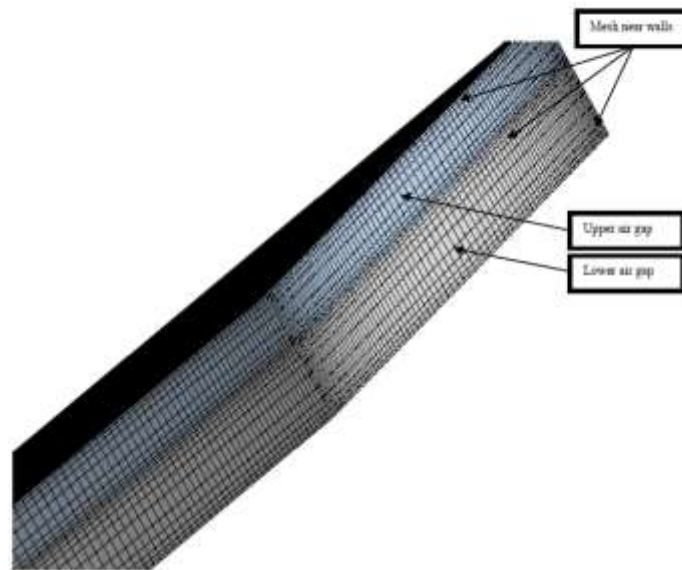


Figure 3. *The computational grid for the air gap spacing*

To predict the heat losses from the solar collector, the velocity and temperature of the air in the gap spacing and the temperature of the upper and lower glass covers require evaluation, since the heat loss depends on these values. The continuity, momentum and energy equations applied to the air in the gaps were solved in a steady state condition using FLUENT software. The pressure-based type solver and the Realizable k- ϵ turbulence model were used. The flow near the walls was treated by using the Non-Equilibrium wall function. The velocity-pressure coupling was treated by using the SIMPLE algorithm and a first order upwind scheme for Momentum, Turbulent Kinetic Energy and Turbulence Dissipation. For the residual, 10^{-4} was used as a convergence criterion for: x-velocity, y-velocity, z-velocity, kinetic energy, epsilon and continuity. For the energy, 10^{-8} was used. The radiation heat transfer between surfaces and to the sky was included in the CFD model. The following two sections describe the radiation model.

RESULTS AND DISCUSSION

Combinations of twelve cases were modelled as the lower air gap, L1, and the upper air gap, L2, were changed. L1 was chosen to be 15, 25 and 40 mm and for each value of L1, L2 was chosen as 15, 25, 35 and 50 mm. Detailed velocity and temperature distributions for the air within the gaps and temperatures of the glass surfaces were obtained. present the velocity vectors for a horizontal plane in the middle of the top gap spacing for the case with L1 equals to 15 mm and L2 equals to 15 and 50 mm, respectively. These figures show that the air velocity increases as the gap spacing increases. However, to facilitate comparison, centre lines (in the z direction) were chosen at which these results are plotted

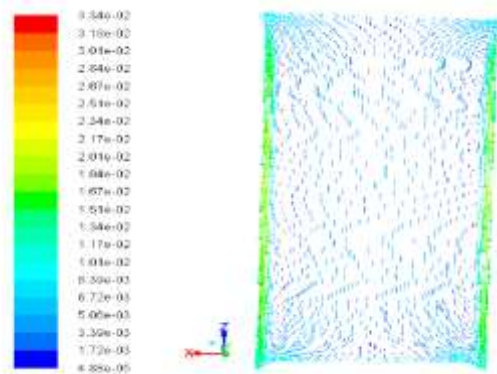


Figure 4. *Velocity vector (m/s) for a horizontal plane in the middle of top gap spacing for L1=L2= 15 mm*

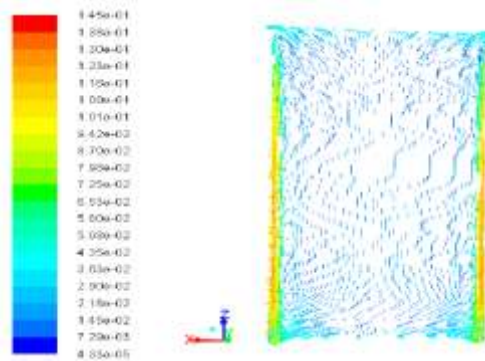


Figure 5. Velocity vector (m/s) for a horizontal plane in the middle of top gap spacing for $L_1=15$ mm and $L_2=50$ mm

For each case of changing L_1 and L_2 , the velocity of the air in the middle of the upper and lower air gaps along the collector (in the z direction) was presented. The figures of these cases are as follows:

1. Figure4. present the air velocity for the case of 15 mm L_1 and 15 mm L_2
2. Figure5. presents the air velocity for the case of 15 mm L_1 and 50 mm L_2

The results showed that as the upper gap spacing was changed, there was no change in the air velocity of the lower gap. The air velocity in the lower gap did not change as the top gap spacing was changed (Figure 6 A). This behaviour was the same for the air velocity in the upper gap which did not change, when the lower gap spacing was changed. The upper and lower air velocity became higher as the upper and lower gap spacing increased, respectively. We can observe that as the lower gap spacing changed from 15 to 40 mm, the velocity in the lower gap spacing increased from 0.009 m/s to 0.016 m/s. Similarly, as the upper gap spacing increased, the air velocity in the upper gap increased

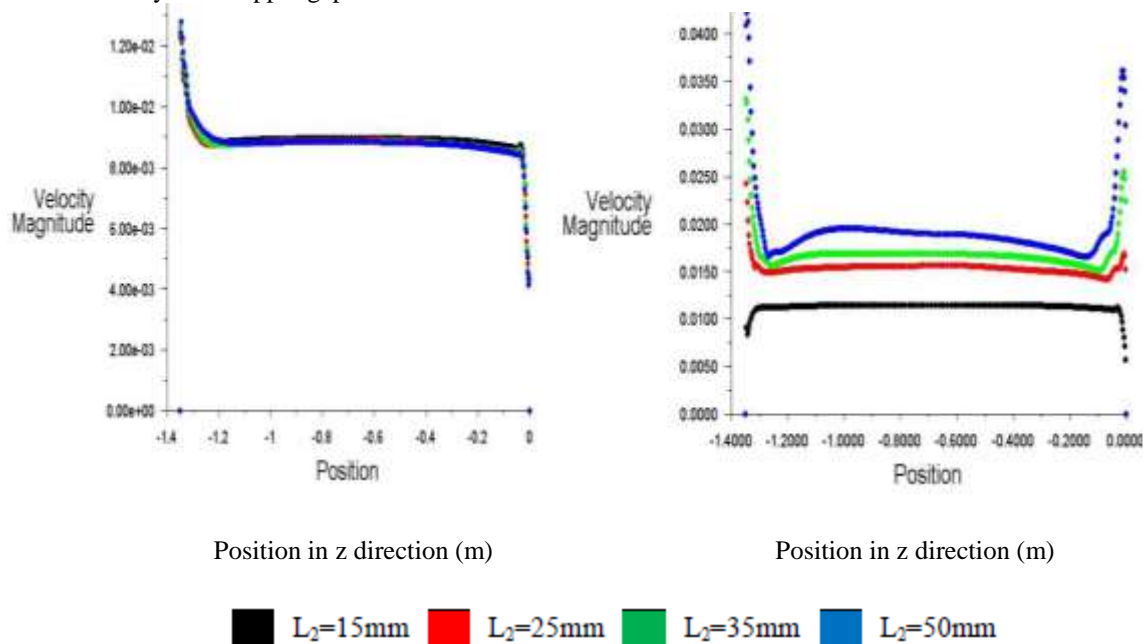


Figure 6.(A) Velocity in the middle of lower gap $L_1=15$ mm and different L_2 , (B) Velocity in the middle of upper gap as L_2 changed and $L_1=15$ mm

CONCLUSION

Due to the increase in the world's population, human development, the increase in individual income, and the aspiration for more comfortable lifestyles, power consumption has increased significantly over the last three

decades resulting in an increase in carbon emissions which was 25.5 GtCO₂ in 2003. Achieving the Millennium Development Goals for 2030 will require that the average carbon emissions for each individual be reduced to 3.7 tCO₂/ year. Thus, the percentage of the energy generated by the renewable sources, including solar energy, must be increased and consumers must be encouraged to use renewable energy rather than other non-environmentally friendly resources. This can be achieved by introducing a more economical and efficient solar collector. ANSYS 13.0-FLUENT software was used to identify the optimum configuration of the indirect heating integrated collector storage solar water heating system which is one of the most economical solar water heating systems. The continuity momentum and energy equations were solved in a steady state condition. The realizable k- ϵ and standard k- ω turbulence models, which are based on the Reynolds-average Navier Stokes equations, were used. The realizable k- ϵ model was used in the optimisation of the air gap spacing. The results for the particular system using the realizable k- ϵ and standard k- ω turbulence models were compared to available experimental results to determine the best model to use in the heat exchanger investigation. The percentage error for the numerical simulation of k- ϵ model was higher than for the k- ω model. The error varied between zero (no errors) and 15 per cent for k- ϵ , and zero to 8.5 per cent for k- ω model. Therefore, the standard k- ω model was used in the heat exchanger investigation.

Minimizing the heat loss and increasing the outlet service water temperature were the main objectives of this study, and were used as a measure of improving the thermal performance. The power required to operate the system was used as a measure of the running cost. The performance of the indirect heating system was enhanced in the following ways:

1. Reduced heat loss from the system
2. Increased outlet temperature
3. Reduced initial cost

ACKNOWLEDGEMENTS

I am very thankful to Department of Mechanical Engineering, BVCEC, Odalarevu for their valuable and insightful guidance.

REFERENCES

1. Gertzos KP, Caouris YG. Optimal arrangement of structural and functional parts in a flat plate integrated collector storage solar water heater (ICSSWH). *Experimental Thermal and Fluid Science* 2008; 32:1105-17.
2. Gertzos KP, Caouris YG, Panidis T. Optimal design and placement of serpentine Heat exchangers for indirect heat withdrawal, inside flat plate integrated collector storage solar water heaters (ICSSWH). *Renewable Energy* 2010; 35:1741-50.
3. Smyth M, Eames PC, Norton B. Integrated collector storage solar water heaters. *Renewable and Sustainable Energy Reviews* 2006; 10:503-38.
4. Kumar R, Rosen MA. Comparative performance investigation of integrated collector-storage solar water heaters with various heat loss reduction strategies. *International Journal of Energy Research* 2011; 35:1179-87.
5. Raupach MR, Marland G, Ciais P, Le Quéré C, Canadell JG, Klepper G, et al. Global and regional drivers of accelerating CO₂ emissions. *Proceedings of the National Academy of Sciences* 2007; 104:10288-93.
6. Gertzos KP, Pnevmatikakis SE, Caouris YG. Experimental and numerical study of heat transfer phenomena, inside a flat-plate integrated collector storage solar water heater (ICSSWH), with indirect heat withdrawal. *Energy Conversion and Management* 2008; 49:3104-15.
7. Kumar R, Rosen MA. Thermal performance of integrated collector storage solar water heater with corrugated absorber surface. *Applied Thermal Engineering* 2010; 30:1764-8.
8. Kreith, F & Bohn, MS 2001, *Principles of Heat Transfer*, 6th edn, Brooks/Cole, USA.
9. Manz, H 2003, 'Numerical simulation of heat transfer by natural convection in cavities of facade elements', *Energy and Buildings*, vol. 35, no. 3, pp. 305-11.
10. Raj Thundil Karuppa R, Pavan P. and Reddy Rajeev D 2012, 'Research Journal of Engineering Sciences' Vol. 1(4), 1-8
11. Mellouli, S, Askri, F, Dhaou, H, Jemni, A & Ben Nasrallah, S 2007, 'A novel design of a heat exchanger for a metal-hydrogen reactor', *International Journal of Hydrogen Energy*, vol. 32, no. 15, pp. 3501-7.

12. Prabhanjan, DG, Raghavan, GSV & Rennie, TJ 2002, 'Comparison of heat transfer rates between a straight tube heat exchanger and a helically coiled heat exchanger', International Communications in Heat and Mass Transfer, vol. 29, no. 2, pp. 185-91.
13. Anderson, JD 1995, Computational fluid dynamics: the basics with applications, McGraw-Hill series in mechanical engineering, McGraw-Hill, New York.
14. Kreith, F 2010, Principles of heat transfer, 7th ed., SI ed. edn, Nelson Engineering, Clifton Park NY
15. Sukhatme S.P. and J.K.Nayak, Solar Energy – Principles of Thermal Collection and Storage, TMH